# Implementation and Verification of Cable Bending Stiffness in MoorDyn

## Preprint

Matthew Hall, Senu Sirnivas, and Yi-Hsiang Yu

*National Renewable Energy Laboratory*

*Presented at the 3rd International Offshore Wind Technical Conference (IOWTC2020)*
*October 18–21, 2020*

**NREL is a national laboratory of the U.S. Department of Energy**
**Office of Energy Efficiency & Renewable Energy**
**Operated by the Alliance for Sustainable Energy, LLC**

This report is available at no cost from the National Renewable Energy Laboratory (NREL) at www.nrel.gov/publications.

Contract No. DE-AC36-08GO28308

**Conference Paper**
NREL/CP-5000-76968
November 2020

# Implementation and Verification of Cable Bending Stiffness in MoorDyn

## Preprint

Matthew Hall, Senu Sirnivas, and Yi-Hsiang Yu

*National Renewable Energy Laboratory*

**Suggested Citation**
Hall, Matthew, Senu Sirnivas, and Yi-Hsiang Yu. 2020. *Implementation and Verification of Cable Bending Stiffness in MoorDyn: Preprint*. Golden, CO: National Renewable Energy Laboratory. NREL/CP-5000-76968. https://www.nrel.gov/docs/fy21osti/76968.pdf.

**NREL is a national laboratory of the U.S. Department of Energy**
**Office of Energy Efficiency & Renewable Energy**
**Operated by the Alliance for Sustainable Energy, LLC**

This report is available at no cost from the National Renewable Energy Laboratory (NREL) at www.nrel.gov/publications.

Contract No. DE-AC36-08GO28308

**Conference Paper**
NREL/CP-5000-76968
November 2020

National Renewable Energy Laboratory
15013 Denver West Parkway
Golden, CO 80401
303-275-3000 • www.nrel.gov

## NOTICE

This work was authored by the National Renewable Energy Laboratory, operated by Alliance for Sustainable Energy, LLC, for the U.S. Department of Energy (DOE) under Contract No. DE-AC36-08GO28308. Funding provided by the U.S. Department of Energy Office of Energy Efficiency and Renewable Energy Water Energy Technologies Office. The views expressed herein do not necessarily represent the views of the DOE or the U.S. Government. The U.S. Government retains and the publisher, by accepting the article for publication, acknowledges that the U.S. Government retains a nonexclusive, paid-up, irrevocable, worldwide license to publish or reproduce the published form of this work, or allow others to do so, for U.S. Government purposes.



*Cover Photos by Dennis Schroeder: (clockwise, left to right) NREL 51934, NREL 45897, NREL 42160, NREL 45891, NREL 48097, NREL 46526.*

# IMPLEMENTATION AND VERIFICATION OF CABLE BENDING STIFFNESS IN MOORDYN

**Matthew Hall,[1] Senu Sirnivas, Yi-Hsiang Yu**
National Renewable Energy Laboratory
Golden, Colorado, USA

## ABSTRACT

*The relatively large motions experienced by floating wind turbines and wave energy converters pose a challenge for power cables, whose internal components provide significant bending resistance and are sensitive to deformation. The behavior and associated design considerations of power cables in these highly dynamic applications make coupled analysis relevant for design.*

*Bending stiffness capabilities have recently been added to the lumped-mass mooring dynamics model MoorDyn to enable simulation of dynamic power cables. MoorDyn is a common modeling choice for floating wind energy simulation (often coupled with OpenFAST) and floating wave energy converter simulation (often coupled with WEC-Sim) but the model's previous line elasticity formulation only considered axial stiffness. To properly capture the dynamics of power cables, a bending stiffness model has been added that approximates cable curvature based on the difference in tangent vectors of adjacent elements. The resulting bending moment is realized by applying forces on adjacent nodes, enabling cable modeling while leaving the underlying lumped-mass formulation unchanged.*

*In this paper, the new bending stiffness implementation is verified in static conditions against analytical solutions and then in a dynamic power cable scenario in comparison with the commercial simulator OrcaFlex. The dynamic scenario uses prescribed motions and includes wave loadings on the cable. Results indicate correct implementation of bending stiffness and show close agreement with OrcaFlex.*

Keywords: cable dynamics, MoorDyn, lumped mass, bending stiffness, dynamic cable.

## 1. INTRODUCTION

Dynamic power cables are a challenging design aspect of floating wind turbines, wave energy converters (WECs), and tidal turbines. Running from a floating device to the seabed, these power cables are required for power transmission and can experience large deformations due to environmental loadings on both the floating device and the cable itself. Keeping the cable bending deformation, axial tension, and fatigue loads within acceptable values is a key design constraint [1].

Dynamic power cables typically contain medium- or high-voltage conductive cores, optical fibers for communication, various protective layers, and twisted wire armoring for structural stiffness and impact protection. Multiple layers of armoring with opposing twist directions are typically used to minimize bend-twist coupling in the cable. Bending stiffness is particularly important for dynamic power cables because they undergo significant wave-induced motion, but can only tolerate a certain minimum bend radius before incurring internal damage. Consequently, accounting for bending stiffness is essential when modeling dynamic power cables in the design process.

Detailed exploration of dynamic power cable design involves (1) simulating the overall dynamics of the cable coupled with the floating system, and then (2) detailed structural analysis of the cable internals subject to the kinematics calculated in the first step [2]. The first step typically uses a medium-fidelity coupled model of the floating system and cable, where the cable is modeled based on gross properties such as linear density and bending stiffness. The second step involves a finite-element analysis of a section of the cable where the internal components—conductor cores, armor wires, etc.—are all represented discretely. The focus in this paper is in the first step, modeling of the overall cable dynamics.

Sophisticated finite-element cable models are readily available in the literature (e.g., [3]), and commercial products exist that provide a variety of fidelity levels for cable analysis (e.g., OrcaFlex and ProteusDS). Limited published examples exist of applying these models to floating wind turbine cable design applications [4]. However, the computational-efficiency demands of models for loads analysis and the utility of open-source models for coupled analysis create a need for efficient, open-source modeling solutions. We are not aware of any preexisting open-source cable model that supports cable bending stiffness.

MoorDyn is a lumped-mass mooring dynamics model that is open source, easy to couple with, and computationally efficient. It is commonly used for floating wind turbine simulation and has a version, MoorDyn F, that is a module in the National Renewable Energy Laboratory's (NREL's) OpenFAST floating wind turbine simulator [5]. It is also used for other applications, such as WECs, and has been coupled with NREL's WEC-Sim simulator [6]. So far, MoorDyn has considered only axial stiffness of line elements, making it suitable for simulating mooring lines but not power cables, where bending stiffness is critical.

This paper presents the formulation and implementation of bending stiffness within MoorDyn's existing mooring line dynamics model. We then discuss several validation tests

[1] Contact author: matthew.hall@nrel.gov

performed with the updated model, checking the quasi-static behavior against analytical solutions and comparing a dynamic cable simulation against results from OrcaFlex.

## 2. THEORY AND IMPLEMENTATION

Of the possible formulations for modeling bending stiffness, we selected a simple approach that approximates curvature based on node positions for its compatibility with the existing MoorDyn lumped-mass formulation. This capability is implemented within the existing line object. To connect line ends with other objects rigidly rather than via a pin connection, rod objects are used and the MoorDyn object hierarchy is adjusted.

### 2.1 Bending Stiffness Implementation

MoorDyn discretizes a mooring line, or cable, into $N+1$ point-mass node points connected by $N$ spring-damper elements. Node coordinates are denoted by $\mathbf{r}_i$, where $i$ is the node number. Segments are numbered such that the segment between nodes $i$ and $i+1$ is numbered as $i+\frac{1}{2}$.

The structural aspect of MoorDyn's existing line object dynamics consists of axial stiffness and damping forces calculated along the elements that connect adjacent nodes based on those nodes' relative motions [7]. The magnitude of this force between two adjacent node points, $i$ and $i+1$, is

$$(T+C)_{i+\frac{1}{2}} = E\frac{\pi}{4}d^2\left(E(\epsilon)\epsilon_{i+\frac{1}{2}} + B(\dot{\epsilon})\dot{\epsilon}_{i+\frac{1}{2}}\right) \tag{1}$$

where $E$ is the elasticity modulus, $\epsilon$ is the segment strain, $B$ is a structural damping coefficient, and $\dot{\epsilon}$ is the segment strain rate. $T$ denotes the stiffness force and $C$ denotes the damping force.

The expanded, vector form of the stiffness portion of (1) is

$$\mathbf{T}_{i+\frac{1}{2}} = E\frac{\pi}{4}d^2\left(\frac{1}{l} - \frac{1}{\|\mathbf{r}_{i+1}-\mathbf{r}_i\|}\right)(\mathbf{r}_{i+1}-\mathbf{r}_i) \tag{2}$$

where the tension force is defined as pointing from node $i$ to node $i+1$ along the element tangent vector:

$$\hat{\mathbf{q}}_{i+\frac{1}{2}} = \frac{\mathbf{r}_{i+1}-\mathbf{r}_i}{\|\mathbf{r}_{i+1}-\mathbf{r}_i\|}. \tag{3}$$

Without adding rotational degrees of freedom to MoorDyn's line nodes, implementing a bending moment entails applying transverse forces on the nodes, perpendicular to the axial stiffness force.

The bending moment at a given location along the line is calculated as

$$M = EI\kappa \tag{4}$$

where $EI$ is the cable's bending stiffness (the product of elasticity modulus and cross-sectional moment of inertia) and $\kappa$ is the local cable curvature (defined as the reciprocal of the local bend radius). Axisymmetric bending stiffness is assumed. Furthermore, torsion is neglected, which avoids the need for additional tracking of cable kinematics.

The curvature at a given node along a line or cable is approximated based on the half-lengths and tangent vectors of the two adjacent cable segments, as depicted in Figure 1. The cosine of the angle between two adjacent segments can be calculated as

$$\cos\alpha = \hat{\mathbf{q}}_{i-\frac{1}{2}} \cdot \hat{\mathbf{q}}_{i+\frac{1}{2}}. \tag{5}$$

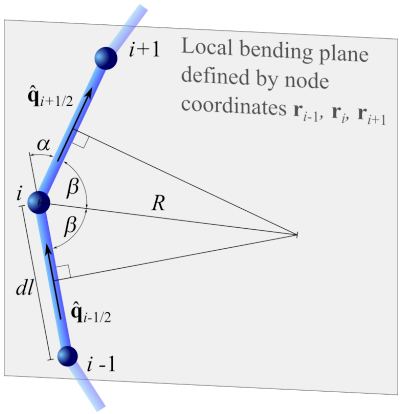


**FIGURE 1:** CURVATURE REPRESENTATION IN MOORDYN

Based on Figure 1, the curvature at node $i$ is

$$\kappa_i = \frac{1}{R} = \frac{2}{dl}\cos\beta = \frac{2}{dl}\cos\left(\frac{\pi-\alpha}{2}\right). \tag{6}$$

Applying some trigonometric identities yields a computationally efficient local curvature calculation:

$$\kappa_i = \frac{2}{dl}\sqrt{\frac{1-\hat{\mathbf{q}}_{i-\frac{1}{2}}\cdot\hat{\mathbf{q}}_{i+\frac{1}{2}}}{2}} \tag{7}$$

where $dl$ is the uniform cable element unstretched length.

With the curvature calculated and bending stiffness provided by the user, the local bending moment magnitude, $M$, is known from (4). What remains is to represent this bending moment via forces applied on the nodes. This moment is realized in MoorDyn as an equivalent set of forces on the node and its two neighboring nodes, as shown on the left side of Figure 2.

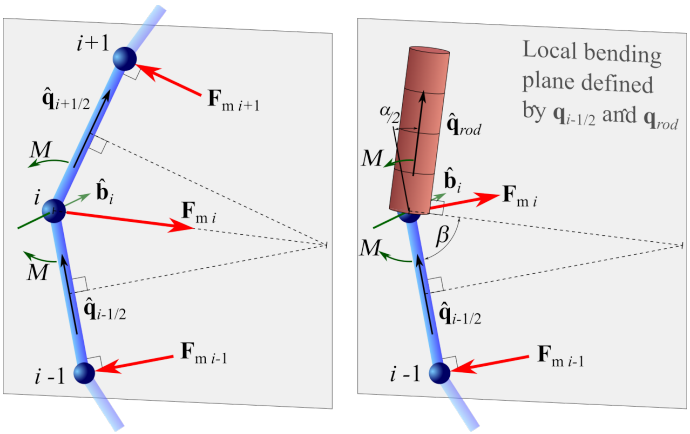


**FIGURE 2:** FORCES APPLYING BENDING MOMENT ALONG CABLE (LEFT) OR AT END ATTACHED TO ROD (RIGHT)

Unit vector $\hat{\mathbf{b}}_i$ is the axis of curvature at node $i$ and can be calculated as

$$\hat{\mathbf{b}}_i = \frac{\hat{\mathbf{q}}_{i-\frac{1}{2}} \times \hat{\mathbf{q}}_{i+\frac{1}{2}}}{\left\| \hat{\mathbf{q}}_{i-\frac{1}{2}} \times \hat{\mathbf{q}}_{i+\frac{1}{2}} \right\|}. \tag{8}$$

The bending moment can be realized by applying a force on node $i$-1 of magnitude $F_{M\,i-1} = M/dl$ and direction $\hat{\mathbf{q}}_{i-\frac{1}{2}} \times \hat{\mathbf{b}}_i$, and a force on node $i$+1 of magnitude $F_{M\,i+1} = M/dl$ and direction $\hat{\mathbf{q}}_{i+\frac{1}{2}} \times \hat{\mathbf{b}}_i$. When there is no curvature, (8) is undefined, so this zero-moment case is handled separately.

Applying these forces, $\mathbf{F}_{\mathrm{M}\,i-1}$ and $\mathbf{F}_{\mathrm{M}\,i+1}$, on the adjacent nodes provides the desired moment about node $i$ but it also results in the addition of a nonphysical net force. Accordingly, an opposing force must be applied on node $i$ to neutralize the net force:

$$\mathbf{F}_{\mathrm{M}\,i} = -(\mathbf{F}_{\mathrm{M}\,i-1} + \mathbf{F}_{\mathrm{M}\,i+1}) \tag{9}$$

This approach allows bending stiffness to be included in MoorDyn line objects without any change to the line state vector or other load calculations.

### 2.2 End Connection Logistics

Lines or cables in a MoorDyn simulation can be given bending stiffness without requiring any change to the model setup or connection behavior. However, this approach results in pinned end connection behavior, which is not appropriate for simulating a dynamic power cable.

To provide a fixed (not pinned) connection capability, rod objects are used. Rods, along with bodies, are new object types introduced in MoorDyn v2 to expand the configurations that MoorDyn can simulate [8]. Rods are rigid six-degree-of-freedom cylindrical bodies that use the same external load physics as lines but have no internal forces. Rods have a connection point at the center of each end, to which lines can be attached.

When a line with nonzero bending stiffness is attached to a rod end, MoorDyn considers this a fixed rather than pinned attachment. The line's end node is coincident with the rod's end node, and a bending moment is enabled at this point. The curvature and bending moment are based on *double* the angle between the line's end segment and the rod's axis, as illustrated by the right side of Figure 2. In other words, (7) is replaced by

$$\kappa_i = \frac{4}{dl}\sqrt{\frac{1 - \hat{\mathbf{q}}_{i-\frac{1}{2}} \cdot \hat{\mathbf{q}}_{rod}}{2}} \tag{10}$$

where $\hat{\mathbf{q}}_{rod}$ is the unit vector along the rod's axis. Imagining a rod inserted along a cable, the approach of (10) results in a consistent cable curvature as the rod length approaches zero.

The signs in (10) match the arrangement shown in Figure 2. Attachments at opposite ends of a line or rod are handled by a straightforward sign reversal. Because rods can be attached to any body object in MoorDyn, including a platform body representing MoorDyn's coupling with an external program, cable ends can be attached at any orientation to any object in MoorDyn without restriction.

The other essential capability for supporting cable dynamics is to allow changes in properties over a cable length. This is also accomplished by the approach of attaching to rods. In this case, a zero-length rod object is used to join two cables with different properties. This approach preserves the bending stiffness behavior across the transition between different cable segments.

## 3. VERIFICATION

To verify the new cable bending stiffness capabilities in MoorDyn, steady state results are compared against analytic beam bending solutions, and a dynamic simulation is compared against results from the commercial simulator OrcaFlex [9].

### 3.1 Static Verification and Convergence Check

Bending stiffness calculations can be verified most simply by performing static deflection tests. Figures 3 and 4 show comparisons between MoorDyn simulations of a 10-m cantilevered cable and the analytical solution for linear beam deflection under a point load at its end. The cable in MoorDyn has a bending stiffness of 2 MN-m$^2$, along with a mass of 100 kg/m and a diameter of 0.3525 m, in order to achieve neutral buoyancy to match the analytical solution. Cables with 2, 4, 6, and 8 segments are simulated, and the results show excellent convergence to the analytical solution as the number of segments increases. This verifies that the bending stiffness implementation is accurate for these curvature ranges.

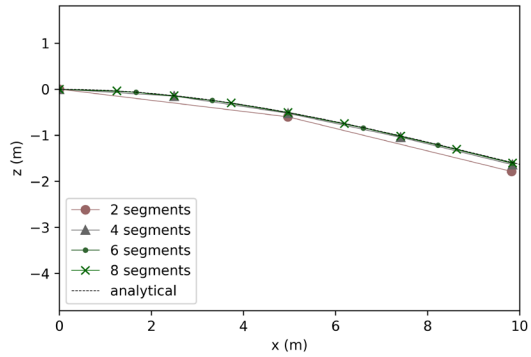


**FIGURE 3:** CABLE DEFLECTION UNDER 1,000 KG END MASS

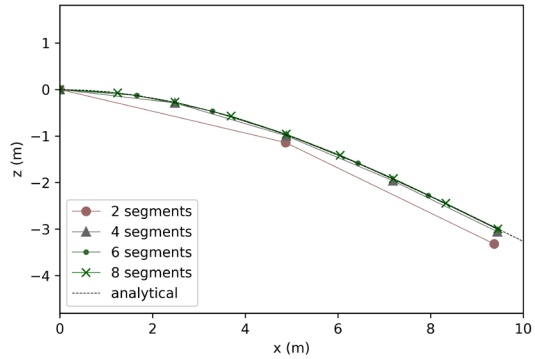


**FIGURE 4:** CABLE DEFLECTION UNDER 2,000 KG END MASS

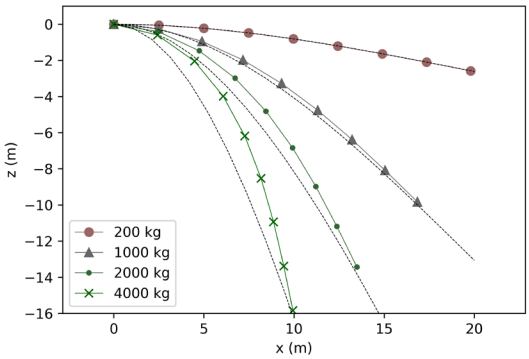


**FIGURE 5:** CABLE DEFLECTION FOR VARYING END LOADS

Figure 5 shows a more extreme case of a 20-m version of the cable, under four different end loads. The varying curvatures show reasonable behavior of the cable bending model under larger bending loads, though this degree of bending is well beyond the assumptions of the linear analytical model.

### 3.2 Dynamic Convergence Check

In addition to static verification, it is worth checking that the overall dynamic model integrates the bending stiffness forces as expected. Figure 6 shows time series of the cable end settling into its equilibrium deflection when initialized undeflected, for cases corresponding to Figure 3. These dynamic results also show convergence as the number of segments increases.

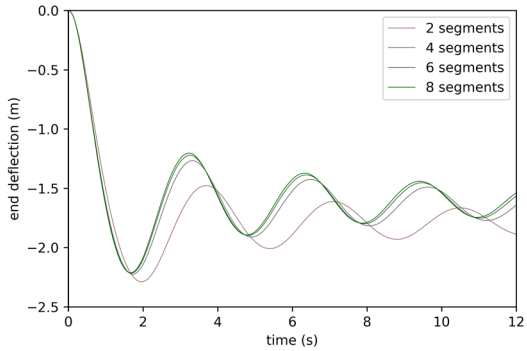


**FIGURE 6:** CABLE END DEFLECTION DECAY DYNAMICS

### 3.3 Dynamic Cable Scenario

To test the full set of new capabilities (including coupling of different cable segments) in a more realistic scenario, we simulated a dynamic power umbilical for a WEC in large waves and compared the results against a corresponding OrcaFlex simulation. We used the Reference Model 3 (RM3) WEC design and an umbilical cable developed for it previously [10].

The cable umbilical consists of three segments in series: (1) a 57-m cable segment that attaches to the WEC, (2) a 25-m buoyancy section the provides a lazy-wave cable profile, and (3) a 55-m cable segment that comes to rest on the seabed and whose end is fixed at a radius of 105.1 m from the device centerline.

An illustration of the device setup in OrcaFlex is shown in Figure 7, and the cable properties are provided in Table 1.

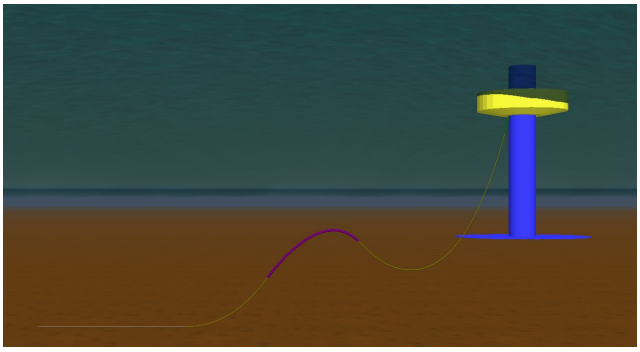

**FIGURE 7:** RM3 WITH CABLE UMBILICAL IN ORCAFLEX

**TABLE 1:** CABLE SEGMENT PROPERTIES

| Cable section | 1 | 2 | 3 |
|---|---|---|---|
| Unstretched length (m) | 57 | 25 | 55 |
| Effective diameter (mm) | 176 | 559 | 176 |
| Linear density (kg/m) | 77.3 | 184.5 | 77.3 |
| Axial stiffness (MN) | 751 | 751 | 751 |
| Bending stiffness (kN-m$^2$) | 11.71 | 11.71 | 11.71 |
| Transverse drag coefficient | 1.2 | 1.2 | 1.2 |
| Transverse added mass coef. | 1.0 | 1.0 | 1.0 |

The simulation scenario features a JONSWAP wave spectrum with a peak period of 14.5 s and significant wave height of 8.25 m. We oriented the cable opposite the direction of wave

propagation, with the anchor point ahead of the device. Motions of the RM3 WEC were taken from previous WEC-Sim simulations with mooring lines but without a power cable. These body motions were then used in OrcaFlex and MoorDyn to drive the cable motion. This uncoupled approach keeps the cable end motion independent from the cable dynamics, enabling a more controlled comparison of cable models.

The OrcaFlex simulation used the prescribed body motions and the cable properties already discussed and included wave kinematics in the calculation of cable loads. Torsion was not included. The model setup included a tapered 4-m-long bend stiffener to reduce bending at the cable attachment point.

The MoorDyn simulation was set up to match the OrcaFlex simulation, with several exceptions. The tapered bend stiffener could not be modeled and was instead roughly approximated by increasing the bending stiffness of the first 4 m of cable to 60 kN-m$^2$. The seabed stiffness coefficient was lowered to reduce seabed-contact tension transients. The cables were discretized with an element length of 1 m, and a time step of 100 µs was used to avoid instabilities. Like OrcaFlex, the MoorDyn simulation used prescribed end-point kinematics and included wave kinematics in the calculation of hydrodynamic loads on the cable. Both simulations were run for 600 s.

Figure 8 shows snapshots of the cable profile at three points during the simulation, comparing the OrcaFlex- and MoorDyn-predicted results. The behavior of the buoyancy section and clear effects from line dynamics are visible in both sets of results. The profiles agree very well between models, with the only significant deviation occurring at the attachment point. This deviation reflects the bend stiffener that was modeled in the OrcaFlex simulation but not in the MoorDyn simulation.

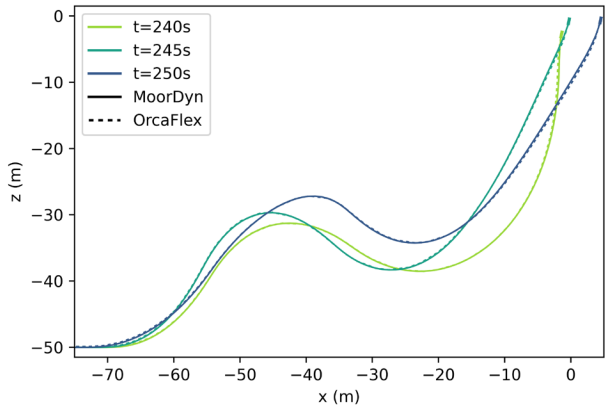


**FIGURE 8:** CABLE PROFILE SNAPSHOTS FROM MOORDYN (SOLID) AND ORCAFLEX (DASHED)

Figure 9 shows the tension along the cable arc length at the same time instances as in Figure 8, again comparing results from both models. The arc length is measured from the upper cable attachment point. Agreement between models is very good, with the largest differences at the attachment point. Peak tensions occur at the junctions between the different cable segment types, as is expected, and these peaks agree very closely.

Figure 10 shows curvature snapshots along the cable arc length. There is good agreement over most of the cable length, but the curvature difference caused by the bend stiffener in the OrcaFlex simulation is very clear.

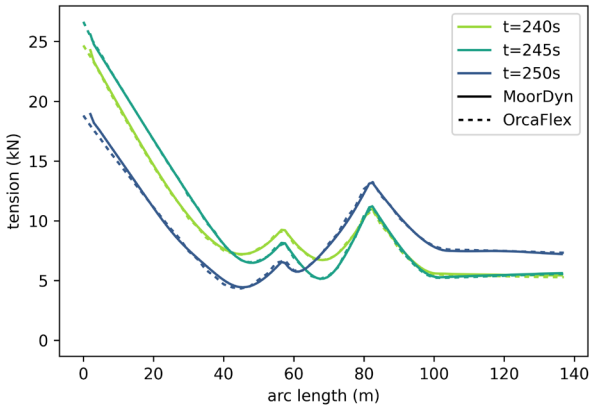


**FIGURE 9:** TENSION SNAPSHOTS OVER CABLE LENGTH

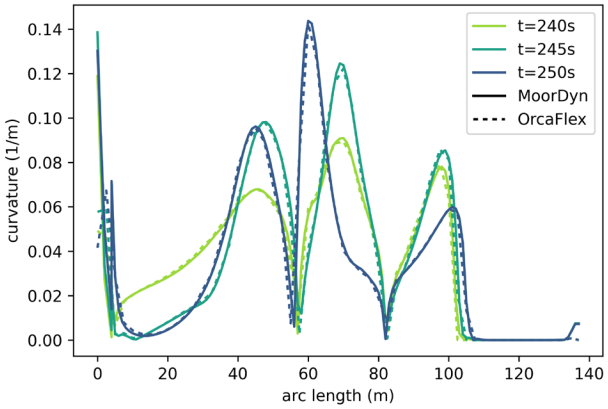


**FIGURE 10:** BENDING SNAPSHOTS OVER CABLE LENGTH

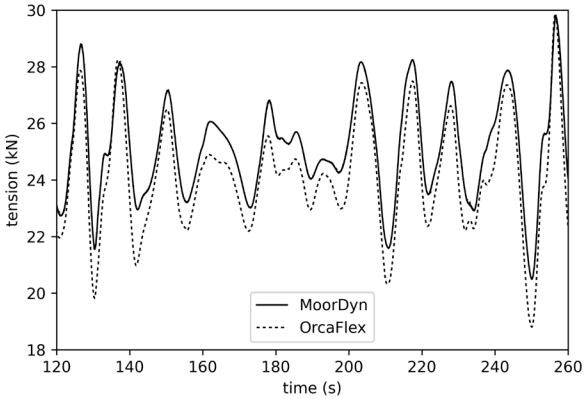


**FIGURE 11:** CABLE ATTACHMENT POINT TENSION

Figure 11 shows time series of the tensions at the cable's attachment point to the WEC from both MoorDyn and OrcaFlex. Consistent with other differences observed at the cable attachment point, some differences in the tension are visible,

although the overall amplitudes and phases agree quite well. There is a small but consistent offset between the results, with MoorDyn predicting slightly greater tensions. This may be a result of the differences in how the bend stiffener was modeled. In OrcaFlex, the tapered bend stiffener added diameter and therefore buoyancy to the cable. In MoorDyn, the bend stiffener was only modeled by an increase in stiffness, meaning there was no buoyancy increase and therefore a greater effective cable weight than in OrcaFlex.

Overall, the comparison between MoorDyn and OrcaFlex results shows that MoorDyn models dynamic cable behavior well, capturing the key physical phenomena very similarly to OrcaFlex. The close agreement of instantaneous distributed tensions and curvatures over the cable length indicates that both models agree very closely in the calculation of not only bending stiffness but also hydrodynamic loads. Wave loading has a significant effect on cable dynamics in the scenario simulated, and the close agreement means that matching of wave kinematics and wave loads was successful. This opens the door to further close comparison of other scenarios between models.

## 4. CONCLUSION

To enable simulation of dynamic power cables, the lumped-mass mooring line model MoorDyn has been expanded to include bending stiffness in its line model. We implemented a simple formulation that uses adjacent segment orientations to calculate local cable curvature, and then applies a set of three forces to realize the resulting bending moment.

The implementation was verified in a static sense against analytic solutions for beam bending. The results show excellent agreement and close convergence to the solution with a relatively coarse discretization of just several elements per cable. Good discretization convergence is also seen in dynamic decay tests, indicating that the correct discretization of dynamics has not been affected by the new bending stiffness term.

To verify the dynamics in a more applicable situation, we ran simulations of a three-segment cable umbilical attached to a wave energy device in OrcaFlex. The end point kinematics are used to drive cable motions in a comparable MoorDyn simulation. Comparison of the results from both tools shows very close agreement in motions and loads over the cable length, with some small differences that can be explained by known differences in the model setup. The level of agreement verifies the implemented representation of cable bending stiffness as well as the calculation of wave loads along the cable.

Once further verifications are completed, the new bending stiffness capabilities in MoorDyn will be ready for simulating a wide range of cable and mooring system scenarios.

## ACKNOWLEDGEMENTS

This work was authored by the National Renewable Energy Laboratory, operated by the Alliance for Sustainable Energy, LLC, for the U.S. Department of Energy (DOE) under Contract No. DE-AC36-08GO28308. Funding provided by the U.S. Department of Energy Office of Energy Efficiency and Renewable Energy Water Power Technologies Office. The views expressed in the article do not necessarily represent the views of the DOE or the U.S. Government. The U.S. Government retains and the publisher, by accepting the article for publication, acknowledges that the U.S. Government retains a nonexclusive, paid-up, irrevocable, worldwide license to publish or reproduce the published form of this work, or allow others to do so, for U.S. Government purposes.

## REFERENCES

[1] P. R. Thies, L. Johanning, and G. H. Smith. 2012. "Assessing mechanical loading regimes and fatigue life of marine power cables in marine energy applications," *Proceedings of the Institution of Mechanical Engineers, Part O: Journal of Risk and Reliability*, vol. 226, no. 1, pp. 18-32.

[2] J.-M. Leroy, Y. Poirette, N. B. Dupend, and F. Caleyron. 2017. "Assessing Mechanical Stresses in Dynamic Power Cables for Floating Offshore Wind Farms," in *Proceedings of the 36th International Conference on Ocean, Offshore and Arctic Engineering*, Trondheim, Norway.

[3] B. Buckham, F. R. Driscoll, and M. Nahon. 2004. "Development of a Finite Element Cable Model for Use in Low-Tension Dynamics Simulation," *Journal of Applied Mechanics*, vol. 71, no. 4, pp. 476-485.

[4] M. U. T. Rentschler, F. Adam, and P. Chainho. 2019. "Design optimization of dynamic inter-array cable systems for floating offshore wind turbines," *Renewable and Sustainable Energy Reviews*, vol. 111, pp. 622-635.

[5] M. T. Andersen, F. T. Wendt, A. N. Robertson, J. M. Jonkman, and M. Hall. 2016. "Verification and Validation of Multisegmented Mooring Capabilities in FAST v8," in *Proceedings of the 26th International Offshore and Polar Engineering Conference*, Rhodes, Greece.

[6] S. Sirnivas, Y.-H. Yu, M. Hall, and B. Bosma. 2016. "Coupled Mooring Analysis for the WEC-Sim Wave Energy Converter Design Tool," in *Proceedings of the 35th International Conference on Ocean, Offshore and Arctic Engineering*, Busan, South Korea.

[7] M. Hall and A. Goupee. 2015. "Validation of a lumped-mass mooring line model with DeepCwind semisubmersible model test data," *Ocean Engineering*, vol. 104, pp. 590-603.

[8] M. Hall. 2020. "MoorDyn V2: New Capabilities in Mooring System Components and Load Cases," in *Proceedings of the 39th International Conference on Ocean, Offshore and Arctic Engineering*, virtual conference, online.

[9] "OrcaFlex Manual." Orcina Ltd. Available: http://www.orcina.com/SoftwareProducts/OrcaFlex/Documentation/OrcaFlex_US_paper_size.pdf.

[10] B. Ballard, Y.-H. Yu, J. Van Rij, and F. R. Driscoll. 2020. "Umbilical Fatigue Analysis for a Wave Energy Converter," in *Proceedings of the 39th International Conference on Ocean, Offshore and Arctic Engineering*, virtual conference, online.